# The efficacy and mechanism of platelet-rich plasma on the myogenic differentiation process of adipose-derived stem cell: A bioinformatics and experimental study

**Xiaochen Wang**
Wuxi Ninth People's Hospital
**Wenyong Fei**
Northern Jiangsu People's Hospital
**Mingsheng Liu**
Dalian Medical University
**Fanglin Shen**
Fudan University
**Yu Liu** ( wxsjyly@163.com )
Wuxi Ninth People's Hospital
**Sanjun Gu**
Wuxi Ninth People's Hospital

**Research Article**

**Keywords:** platelet-rich plasma, adipose mesenchymal stem cells, myogenic differentiation, CCL-2, mitophagy

**Posted Date:** May 25th, 2022

**DOI:** https://doi.org/10.21203/rs.3.rs-173133/v2

## Abstract

# Background

Platelet-rich plasma (PRP) can effectively treat injury of musculoskeletal system, but there is no consensus on whether it can effectively promote the myogenic differentiation of adipose mesenchymal stem cells.

# Methods

Dataset of PRP in the treatment of musculoskeletal injury was obtained by GEO database and the key pathways of PRP were identified by KEGG enrichment analysis. PPI network was constructed by Cytoscape and core gene was identified by the MOCODE. ADSCs were clutivated in vitro and 5-Aza combined PRP were added. MTT were performed to determine the cell viability. Cell senescence was detected by β-galactosidase. Immunofluorescence staining was used to detect the expression of MHC and MyoD. Core gene expression was detected by RT-PCR. Mito-tracker staining and transmission electron microscope were performed respectively.

# Results

GSE70918 was obtained and 148 differentially expressed genes were obtained. KEGG analysis showed the differential genes were enriched in GPCR-related pathways. CCL2 was set as core gene. MTT showed that PRP significantly increase the viability of ADSCs and the IC50 was 19.4 μmol/L. After the addition of 5-Aza combined with PRP, β-galactosidase showed the number of senescent cells decreased significantly, immunofluorescence staining showed the expression of MHC and MyoD increased significantly, RT-PCR showed the expression of CCL-2 decreased significantl, mito-tracker staining showed the number of mitochondria increased and transmission electron microscopy showed the number of mitophagy increased significantly.

# Conclusion

PRP can effectively protect the viability of ADSCs, promote myogenic differentiation efficiency and promote mitophagy. The above functions may be caused by inhibiting the expression of CCL-2.

## Introduction

The atrophy of the muscular tissue has been an issue perplexed orthopediscs, aimed at repairing damaged tissues in surgery, for the postoperative complications it takes. For example, rotator cuff tear, a chronic disease despaired the supraspinatus, owns a high re-tear rates of 94%[1] for the muscular atrophy

as a main cause from Takashi Hashimoto, MD study[2]. As for the Duchenne Muscular Dystrophy, originated in the muscular atrophy, there still remains no effective method to hold back the progression of this disease[3]. Muscular tissue, originating from the mesoderm of our embryo, barely owns the regenerative ability for the terminal differentiating forms they are. Therefore, inventing an effective method to regenerate the damaged muscular tissue is urgently needed.

Promisingly, the stem cells, which own multidirectional differentiating abilities, have been expected to regenerate the damaged tissue and guide the clinical treatments. The Adipose-derived stem Page 3/17 cells was firstly published in 2002 and they proved this type of stem cells owns multilineage mesodermal differentiating potential which includes the muscular tissue[4]. From the previous studies, the adipose mesenchymal stem cells (ADSCs) can be induced into myocyte with various inductions as 5-Aza, boron, Cyclic uniaxial stress, etc[5–7]. And among them, the 5-Aza was set as a relative stabilized induction with specific myogenic differentiation ability not only in the ADSCs but also in the other mesenchymal stem cells (MSCs). However, during the induction, there always exists the reduction of cell proliferation ability because of the toxic effect of the inducers. The previous study showed that the cell viability was significantly reduced after 5-Aza induction. Therefore, an effective agent to prevent the toxic effect during induction is urgently needed.

Platelet-rich plasma (PRP), concentrated and collected from autologous platelet, is used in the field of stimulating tissue growth for the capacity of promote the proliferating ability. The PRP realizes its effects mainly for the growth factors it contains which is critical to tissue regeneration, cellular recruitment and angiogenesis. In the previous research, PRP contains the ability of inducing the stem cells toward ADSC osteogenesis differentiation[8]. Meanwhile, PRP, combined with a TGF-β inhibitor, turned to myogenic differentiation in Robi research[9]. As for the Michael J. McClure study, it reveals that PRP owns the ability of up-regulating the myogenic regulatory factors (MRFs) which represent the inchoate myogenic differentiation and down-regulate the MRFs which represent the terminal myogenic differentiation[10]. Whether PRP owns positive or negative effects on the myogenic differentiating process of ADSCs after the induction of 5-Aza is still a mystery.

# Materials And Methods

### Microarray data obtained:

Through the research from the Gene Expression Omnibus (GEO) database, the gene expression profile, GSE 70918 (GPL 19271, Affymetrix Rat Gene 2.1 ST Array) was obtained. In this profile, comprising 4 samples, of which 2 were cultivated with PRP and the other 2 samples were cultivated with platelet-poor plasma (PPP). All of the 4 samples were included into this study.

### Identification of differently expressed genes (DEGs)

The GEO2R tool was used to analyze the differently expressed genes. And the threshold of the DEGs in our study was set as |logFC|>1 and *p*-value < 0.05.

### (Protein-protein interaction) PPI network construction and module selection

The PPI network based on commonly differentially expressed genes was constructed by Search Tool for the Retrieval Interacting Genes (STRING) database. The Cytoscape (version 3.8.0) was used to analyze and visualize the correlations among genes. Molecular Complex Detection (MCODE; version 1.31) was used to determine the top 3 correlated gene modules.

### KEGG pathway enrichment analysis construction

The Database for Annotation, Visualization and Integrated Discovery (DAVID, version 6.8) was used to analyze the KEGG functional enrichment based on the DEGs.

### Cell viability evaluated by MTT test

The passage-3 ADSCs were digested and diluted, and the mixture was transferred to a 96-well culture plate at 100 μL cell suspension per well and incubated at 37 ℃, in a 5% $CO_2$-saturated humidity float tank for 24 hours. 5-Aza was then added to each well containing ADSCs at concentrations of 0, 10, 20, 30, 40 μmol/L. ADSCs group were labeled groups A, B, C, D and E. Following incubation under the same conditions as before for 24 hours, we added 50 μL MTT solution to each well and incubated again under the same conditions for another 4 hours, terminating the reaction of each well by aspirating the culture medium. To each well was added 150 μL DMSO solution after terminating the 4 hours of incubation, with the plate placed on the table concentrator. Finally, the absorbance of each well was measured at 550 nm (OD) to detect the cell viability under the induction of different concentrations of 5- Aza.

### Aging-associated β-galactosidase (SA- β-gal) staining

According to the instructions of the reagent, the aging β-galactosidase staining kit (CST Company) was used to detect the activity of SA- β-gal in ADSCs. SA- β-gal positive cells were quantified as a percentage of the total number of cells analyzed.

### Immunohistochemical staining and Semi-quantitative analysis

First, we digested and diluted the cells from each group 9 days after induction; then we added 1 mL of the solution to each well of the 12-well culture plate that had a cell slide placed in every well in advance. We next extracted the slides from each well after culturing at 37 ℃ in a 5% $CO_2$-saturated humidity incubator for 24 hours. We washed the slides once with 300 μL phosphate buffer solution (PBS) and did not remove the liquid for 5 minutes until the cells were saturated. Next, we added 150 μL 4% paraformaldehyde fixative to every slide and left them undisturbed for 30 minutes before adding 150 μL 0.1% Triton x-100 to each and left at room temperature for 3 minutes. We washed the slide 3 times with 300 μL PBS, each washing process lasting 5 minutes. The ensuing step was to drop 200 μL 5% blocking

solution (BSA) to each slide and incubate in a 5% $CO_2$ incubator for 1 hour. Each slide was incubated overnight at 4 ℃ after being mixed with 150 μL α-SMA (1:200) diluted with 1% BSA. The slides were washed with 300 μL PBS 5 times the following day, each washing process lasting 5 minutes. 150 μK of the secondary antibody (1:200) diluted with 1% BSA was then added to each slide after the slides were blocked at room temperature with 200 μK 1% BSA for 15 minutes. Next, we washed the slides 5 times with 300 μL PBS for 5 minutes each time. 150 μL Hoechst33258 stain (C1011 Beyotine, China) was added to each slide in a dark environment and incubated for 30 minutes at room temperature. Finally, we observed the cells under a fluorescence microscope, photographed, and stored them.

### RT-PCR

Intracellular total RNA extraction: Pancreatic enzymes were used to digest the cells that were collected after centrifuging the liquid in the flask. Next, equal volumes of Trizol lysate were added to enable the collected cells to split and decompose. The schizolytic cells were then transferred into another tube without RNA enzymes, and 200 μL pre-cooling chloroform was added per milliliter of Trizol, and the mixture was centrifuged for 15 minutes. The supernatant was absorbed after centrifugation and transferred into another tube without RNA enzymes, where an identical volume of isopropanol was added to the tube, followed by another centrifugation. This later centrifugation yielded RNA sediments that were preserved in a -20 ℃ surrounding for 30 minutes. The sediments were washed with 75% ethyl alcohol and centrifuged for 5 minutes, and the supernatant was discarded after washing and centrifuging the sediments twice. cDNA synthesis: The reverse transcription system was prepared using a reverse transcription kit according to instructions provided in the protocol of the kit.

### Mito-Tracker

After washing with PBS for 2 - 3 times, it was added to M16 culture medium preheated to 37 ℃ and containing 400 nmol/L Mito-Tracker Red. The cells were stained at 37 ℃ for 20 minutes. After staining, the cells of each group were washed with PBS for 2 - 3 times, and the cells of each group were placed on the glass slides, covered with glass slides, and observed and photographed under the fluorescence microscope.

### Transmission electron microscope

The cells of each group cultured for 72 hours were fixed with 2.5% glutaraldehyde and 1% osmium acid, dehydrated with acetone, prepared, lead and uranium were re-stained with 10 minutes, and the autophagosomes were observed and photographed under transmission electron microscope.

### Statistical analysis

Graphpad 8.0.2 and R 4.0.2 were used to perform statistical analysis. Expressed data were shown as mean ± SD. Student's t test was used to evaluate the statistical significance of different 3 groups. The *p* value less than 0.05 was considered as significant.

## Results

# 1. The results of bioinformatics analysis:

Through the analysis of GSE70918 data set, 148 significant differentially expressed genes were obtained. KEGG enrichment analysis showed that the differentially expressed genes were mainly enriched in GPCR-related signal pathway (Fig. 1A). The PPI network (Fig. 1B) was constructed for 148 differentially expressed genes, and the core target was CCL2 (Fig. 1C-D) obtained by the MOCDE plug-in. CCL2 is the key target of GPCR-related signaling pathway.

# 2. The effect of PRP on the activity of ADSC cells:

The results of MTT experiment showed that the activity of ADSCs increased significantly after adding PRP, and the calculated $IC_{50}$ was 19.4 μmol/L (Fig. 2C). The results of β-galactosidase test showed that the number of senescent cells increased significantly when 5-Aza was added to ADSC, and decreased significantly when 5-Aza combined with PRP was added.

# 3. Effect of PRP on myogenic differentiation of ADSCs and expression of CCL-2:

The expression of MHC and MyoD in ADSCs was evaluated by immunofluorescence staining and semi-quantitative analysis. The results showed that the expression level of MHC and MyoD increased when 5-Aza was added, and the expression level of MHC and MyoD further increased when 5-Aza combined with PRP was added ($p < 0.05$) (Fig. 3A-D). Furthermore, the expression level of CCL-2 in each group was detected by RT-PCR, and the results showed that the expression level of CCL-2 in cells increased significantly after the addition of 5-Aza. After the addition of 5-Aza and PRP, the expression of CCL-2 in ADSCs decreased significantly ($p < 0.05$) (Fig. 3E).

# 4. The regulatory effect of PRP on the mitochondrial function of ADSCs:

To further explore the mechanism of PRP protecting cell activity and promoting myogenic differentiation, the changes of morphology and number of mitochondria were detected by mito-Tracker. The results showed that the morphology of mitochondria in cytoskeleton was irregular and the number of mitochondria decreased after adding 5-Aza. After the addition of 5-Aza and PRP, the number of mitochondrial fusion and division increased, and the total number of mitophagy increased significantly ($p < 0.05$). The occurrence of mitophagy was observed by transmission electron microscope (Fig. 4A-B). The results showed that the number of mitophagy decreased significantly after adding 5-Aza, while the number of mitophagy increased significantly after adding 5-Aza combined with PRP (Fig. 4C).

## Discussion

The results of this study showed that the addition of 5-Aza to ADSCs could promote myogenic differentiation, but inhibit cell function and promote the expression of CCL-2 inflammatory factors. After the combination of 5-Aza and PRP, the cell activity was restored and the myogenic differentiation ability was increased. The incidence of mitophagy increased. For more information on the hypotheses of this study, please see Fig. 5.

The ability of skeletal muscle to regenerate is low, and once the defect begins, the treatment is limited, which is a problem for orthopedic physicians and orthopedic surgeons. Adipose stem cells are abundant, easy to obtain, high yield, strong proliferation ability, can paracrine a variety of cytokines, and can differentiate into skeletal muscle myoblasts under specific conditions. Cell therapy based on adipose stem cells and muscle tissue engineering provides a new idea for the repair of skeletal muscle injury. 5-Aza is the main chemical factor that induces myogenic differentiation of adipose stem cells in vitro. By preventing cytosine methylation of newly replicated DNA, 5-Aza activates myogenic genes that were transcribed inactivated. Mizuno et al first used the basic culture medium supplemented with 5-Aza, dexamethasone, hydrocortisone and serum to induce adipose stem cells to differentiate into skeletal myoblasts. However, the differentiation efficiency of 5-Aza was low, and its cytotoxicity was proportional to the concentration. 20 μmol/L 5-Aza could cause 30% cell death. Studies have shown that 10 μmol/L 5-azacytidine can obtain a higher myogenic induction rate and control its cytotoxicity at a lower level. The results of our team show that 10 μmol/L 5-Aza has a certain degree of myogenic differentiation, but it can promote cell senescence and promote the release of inflammatory factor CCL-2.

With the further research, it is shown that a variety of cytokines have a certain role of myogenic differentiation. Vascular endothelial growth factor (VEGF): blocking the expression of vascular endothelial growth factor in adipose stem cells, adipose stem cells can not differentiate into muscle cells[12]. The mechanism may be that vascular endothelial growth factor promotes muscle regeneration by promoting angiogenesis. Insulin-like growth factor 1 (IGF-1): IGF-1 can activate skeletal muscle satellite cells, promote myoblast proliferation and differentiation, increase the level of PI3K, inhibit apoptosis and inflammation, reduce skeletal muscle fibrosis and promote the regeneration of injured skeletal muscle. Transforming growth factor β (TGF-β): TGF-β promotes skeletal muscle fibrosis by re-coding muscle cell genes and inhibiting the expression of myogenic regulatory factors such as MyoD, myf5 and myogenin[16]. Adipose stem cells can regulate the expression of TGF-β and inhibit skeletal muscle fibrosis. All the above factors are the key components of PRP. PRP has played a key role in the treatment of muscle injury, but there are few studies on whether PRP can promote myogenic differentiation. The previous bioinformatics analysis of our team showed that PRP could significantly reduce the expression of inflammatory factor-related pathways, while building a PPI network to find the core target, the results showed that CCL-2 was the key core target. On this basis, the team believes that PRP mainly inhibits inflammation through CCL-2, thus improving cell activity. However, by adding PRP to 5-Aza, the number of senescent cells decreased significantly by β-galactosidase experiment. On this basis, the team believes that 5-Aza combined with PRP can improve cell activity and promote myogenic differentiation of ADSCs. On this basis, the team further detected the changes of myogenic differentiation

ability of cells by immunofluorescence. The results showed that the expression levels of MHC and MyoD were significantly increased after adding PRP. These results suggest that PRP may be involved in the induction of myoblast differentiation.

Previous studies have shown that the occurrence of mitophagy is closely related to muscle mass. The mechanism of mitophagy is related to aging. Studies have confirmed that aging skeletal muscle is often accompanied by the accumulation of impaired mitochondria[18]. In response to mitochondrial fragmentation, decrease of mitochondrial membrane potential and increase of mitochondrial ROS production, mitophagy increased, while mitophagy was damaged in aging skeletal muscle. Firstly, mitochondria are sensitive to the transition of mitochondrial membrane permeability in aging skeletal muscle, and the decrease of mitochondrial membrane potential can effectively induce mitophagy[19]. The regulation of mitochondrial membrane permeability transition is mediated by mitochondrial permeability transition pores. The opening of mitochondrial permeability transition pore can promote the occurrence of mitophagy, while its inhibitor can inhibit the decrease of mitochondrial membrane potential and inhibit the occurrence of mitophagy[20]. Secondly, Parkin and Pink1 proteins are also involved in mitophagy induced by decreased membrane potential[21]. Pink1 is located in the upstream of Parkin, which promotes the translocation of Parkin from cytoplasm to mitochondria and provides Parkin with a signal to selectively degrade damaged mitochondria[22]. Parkin can selectively recruit low membrane potential dysfunctional mitochondria in mammalian cells and selectively eliminate them by autophagosomes. In addition, Parkin can interact with autophagy protein LC3 and induce the formation of autophagosomes in dysfunctional mitochondria. It was found that the level of Parkin protein in skeletal muscle decreased in physically active 70-years-old men[23] and inactive elderly women[24]. It can be seen that mitophagy is related to the occurrence of myopenia. On this basis, the team believes that PRP may promote myogenic differentiation by regulating mitophagy. However, the number and morphology of mitochondria were evaluated by mito-Tracker experiment. The results showed that the number of mitochondria increased significantly after the addition of PRP to 5-Aza. The occurrence of mitophagy was observed by transmission electron microscope (TEM). The results showed that the number of mitophagy bodies increased significantly after PRP was added to 5-Aza.

# Conclusion

The addition of 5-Aza to ADSCs can promote myogenic differentiation, but inhibit cell function and promote the expression of CCL-2 inflammatory factors.

# Declarations

### Ethics approval and consent to participate

This study was approved by ethics of committee of Northern Jiangsu People's Hospital.

### Consent for publish

Not applicable.

### Availability of data and materials

The data used and analyzed during the current study are available from the corresponding author on reasonable request.

### Competing Interest

The authors declare that they have no competing interests.


### Funding

This work was supported by the funds from the Medical and Public Health Technology Innovation and Application Project of Wuxi Science and Technology Bureau (contract number N20202041); the youth talent project of Wuxi health commission (contract number Q202150); Duo-Innovative and Excellent Doctors Project of Wuxi 9th People's Hospital (contract number YB202107).


### Author contributions

Xiaochen Wang. Wenyong Fei. and Mingsheng Liu. Yu Liu. wrote the main manuscript text and Xiaochen Wang. Fanglin Shen. prepared figures 1-5. All authors reviewed the manuscript.

## References


1. Zhang Zhenbin,Nie Pan,Yang Wende et al. Lipopolysaccharide-preconditioned allogeneic adipose-derived stem cells improve erectile function in a rat model of bilateral cavernous nerve injury.[J].Basic Clin Androl, 2022, 32: 5.
2. Shi Zheng-Liang,Fan Zhi-Yong,Zhang Hua et al. Localized delivery of brain-derived neurotrophic factor from PLGA microspheres promotes peripheral nerve regeneration in rats.[J].J Orthop Surg Res, 2022, 17: 172.
3. Ni Hui,Liu Chang,Chen Yuwen et al. MGP Regulates Perivascular Adipose-Derived Stem Cells Differentiation Toward Smooth Muscle Cells Via BMP2/SMAD Pathway Enhancing Neointimal Formation.[J].Cell Transplant, 2022, 31: 9636897221075747.
4. Feng Chen-Ye,Bai Shi-Yao,Li Meng-Lu et al. Adipose-Derived Mesenchymal Stem Cell-Derived Exosomal miR-301a-3p Regulates Airway Smooth Muscle Cells During Asthma by Targeting STAT3.[J].J Asthma Allergy, 2022, 15: 99–110.
5. Hadipour Azam,Bayati Vahid,Rashno Mohammad et al. Aligned Poly(ε-caprolactone) Nanofibers Superimposed on Decellularized Human Amniotic Membrane Promoted Myogenic Differentiation of Adipose Derived Stem Cells.[J].Cell J, 2021, 23: 603–611.
6. Wang Fuke,Yang Guiran,Xiao Yu et al. Effects of Tissue-engineered Bone by Coculture of Adipose-derived Stem Cells and Vascular Endothelial Cells on Host Immune Status.[J].Ann Plast Surg, 2021,

87: 689–693.

7. Xie Yao,Ji Yongli,Lu Yunrui et al. Distinct Characteristics Between Perivascular and Subcutaneous Adipose-Derived Stem Cells.[J].Diabetes, 2022, 71: 321–328.
8. Liu Junjie,Li Fuxingzi,Liu Binjie et al. Adipose-derived mesenchymal stem cell exosomes inhibit transforming growth factor-β1-induced collagen synthesis in oral mucosal fibroblasts.[J].Exp Ther Med, 2021, 22: 1419.
9. Zheng Han,Bai Zhifang,Xu Yongde et al. Effects of Cells Self-aggregation in the Treatment of Neurogenic Erectile Dysfunction With Traditional Single Cell Suspension of Adipose-derived Stem Cells.[J].Urology, 2021, 158: 102–109.
10. Kim Jonghun,Hasegawa Toshio,Wada Akino et al. Keratinocyte-Like Cells Trans-Differentiated from Human Adipose-Derived Stem Cells, Facilitate Skin Wound Healing in Mice.[J].Ann Dermatol, 2021, 33: 324–332.
11. Zhong Hao,Shen Yamei,Zhao Danhui et al. Cell-Seeded Acellular Artery for Reconstruction of Long Urethral Defects in a Canine Model.[J].Stem Cells Int, 2021, 2021: 8854479.
12. Jing Boping,Qian Ruijie,Jiang Dawei et al. Extracellular vesicles-based pre-targeting strategy enables multi-modal imaging of orthotopic colon cancer and image-guided surgery.[J].J Nanobiotechnology, 2021, 19: 151.
13. Qi Yicheng,Liu Wen,Wang Xiangsheng et al. Adipose-derived mesenchymal stem cells from obese mice prevent body weight gain and hyperglycemia.[J].Stem Cell Res Ther, 2021, 12: 277.
14. Liu Shao-Cheng,Bamodu Oluwaseun Adebayo,Kuo Kuang-Tai et al. Adipose-derived stem cell induced-tissue repair or wound healing is mediated by the concomitant upregulation of miR-21 and miR-29b expression and activation of the AKT signaling pathway.[J].Arch Biochem Biophys, 2021, 705: 108895.
15. Kurdi Ban Al-,Ababneh Nidaa A,Abuharfeil Nizar et al. Use of conditioned media (CM) and xeno-free serum substitute on human adipose-derived stem cells (ADSCs) differentiation into urothelial-like cells.[J].PeerJ, 2021, 9: e10890.
16. Kurdi Ban Al-,Ababneh Nidaa A,Abuharfeil Nizar et al. Use of conditioned media (CM) and xeno-free serum substitute on human adipose-derived stem cells (ADSCs) differentiation into urothelial-like cells.[J].PeerJ, 2021, 9: e10890.
17. Wang Chengyuan,Wang Hui,Guo Qianping et al. Bladder muscle regeneration enhanced by sustainable delivery of heparin from bilayer scaffolds carrying stem cells in a rat bladder partial cystectomy model.[J].Biomed Mater, 2021, 16: undefined.
18. Chen Xin,Yang Qiyun,Xie Yun et al. Comparative study of different transplantation methods of adipose tissue-derived stem cells in the treatment of erectile dysfunction caused by cavernous nerve injury.[J].Andrologia, 2021, 53: e13950.
19. Xie Fang,Teng Li,Xu Jiajie et al. Adipose-derived mesenchymal stem cells inhibit cell proliferation and migration and suppress extracellular matrix synthesis in hypertrophic-scar and keloid fibroblasts.[J].Exp Ther Med, 2021, 21: 139.

20. Otsuka Takayoshi,Mengsteab Paulos Y,Laurencin Cato T,Control of mesenchymal cell fate via application of FGF-8b in vitro.[J].Stem Cell Res, 2021, 51: 102155.
21. Wang Liang,Li Huan,Lin Jinfu et al. CCR2 improves homing and engraftment of adipose-derived stem cells in dystrophic mice.[J].Stem Cell Res Ther, 2021, 12: 12.
22. Nakajima Tadahiro,Tada Kaoru,Nakada Mika et al. Facilitatory effects of artificial nerve filled with adipose-derived stem cell sheets on peripheral nerve regeneration: An experimental study.[J].J Orthop Sci, 2021, 26: 1113–1118.
23. Yang Shaojie,Jiang Xia,Xiao Xiong et al. Controlling the Poly(ε-caprolactone) Degradation to Maintain the Stemness and Function of Adipose-Derived Mesenchymal Stem Cells in Vascular Regeneration Application.[J].Macromol Biosci, 2021, 21: e2000226.

# Figures

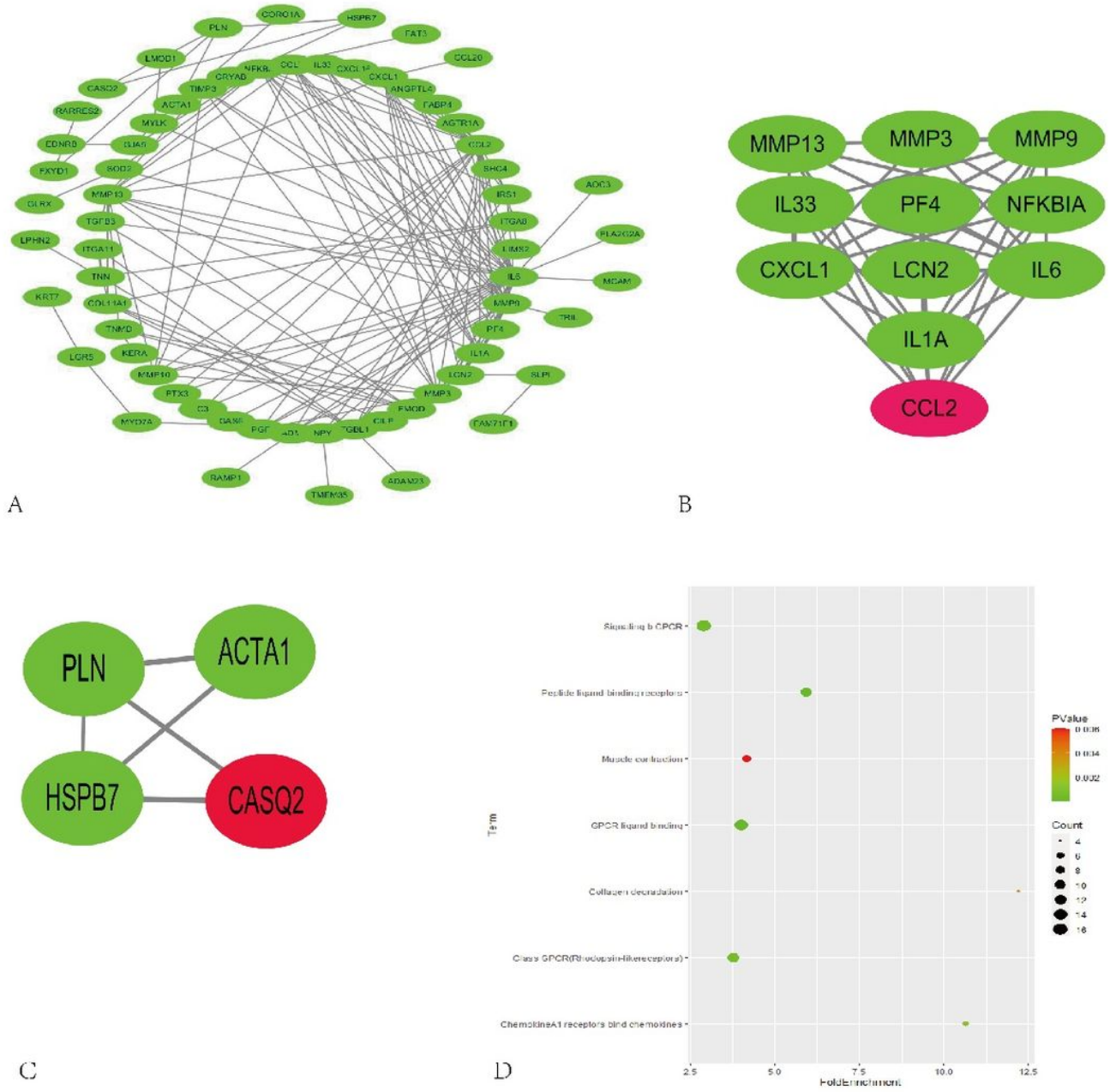


## Figure 1

**The bioinformatics analysis of PRP on muscular cells.** A: PPI network constructed by cytoscape; B, C: MOCODE plug-in to determine the core gene (core genes were stained in red); D: KEGG analysis based on the DEGs.

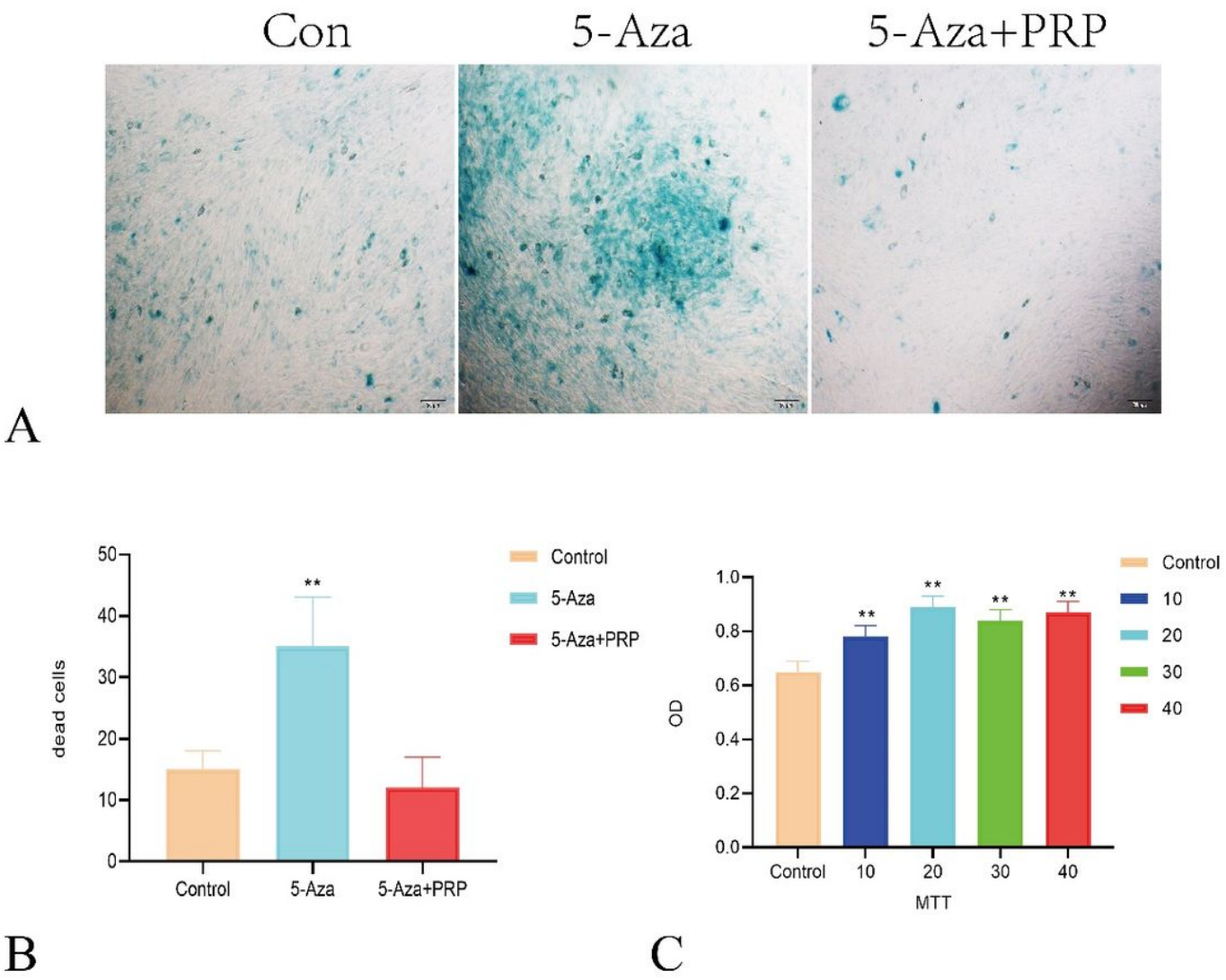


## Figure 2

**The effects of PRP on the cell viability.** A: β-galactosidase test; B: The senescent cells comparisons between control, 5-Aza and 5-Aza combined PRP group; C: MTT to determine the cell viability in ADSCs treated with different concentrations of PRP. ** $p < 0.05$.

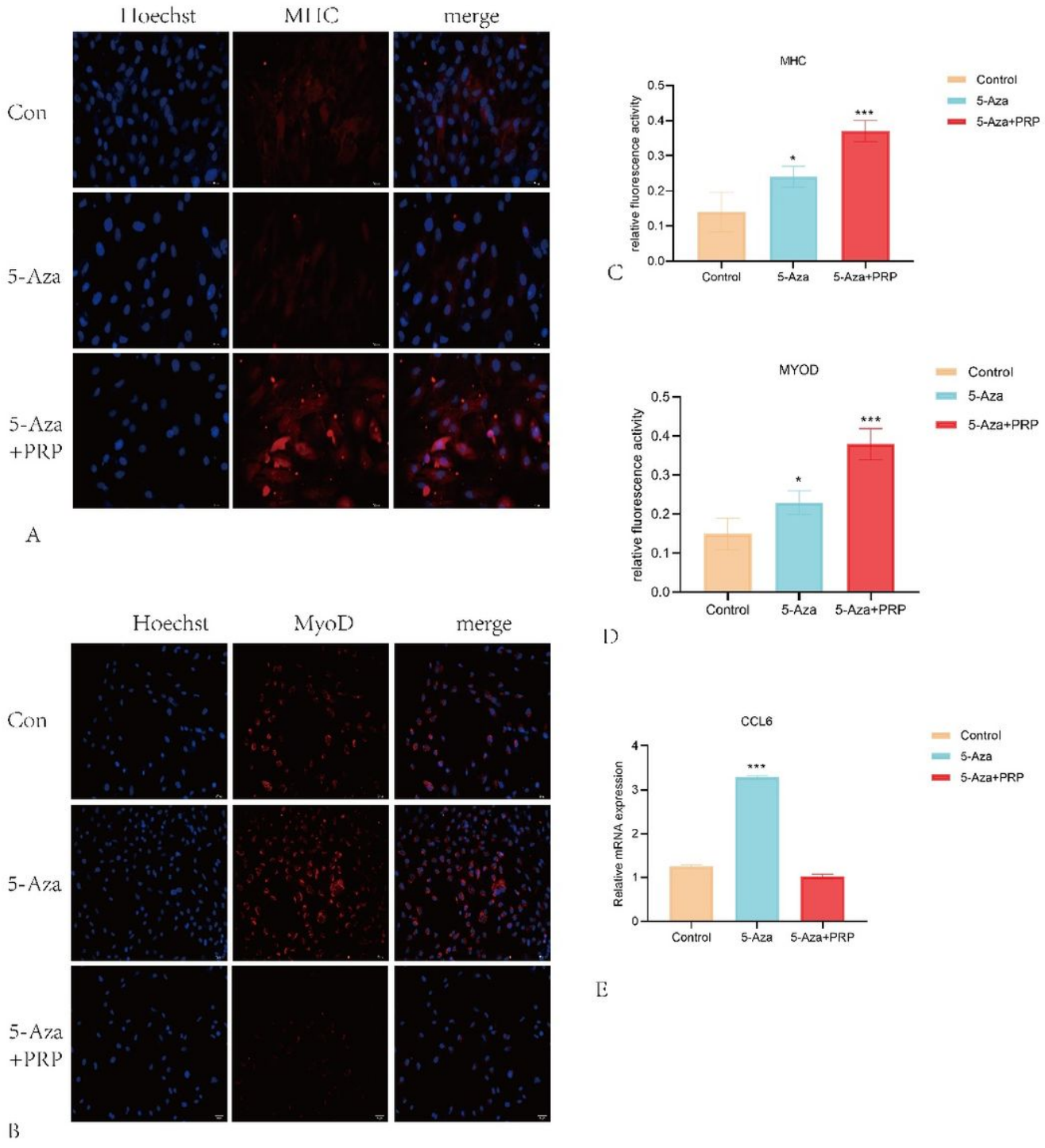


## Figure 3

**Effect of PRP on myogenic differentiation of ADSCs and CCL-2 expression.** A: Immunofluorescence staining to determine MHC expression; B: Immunofluorescence staining to determine MyoD expression; C: Semi-quantitative analysis to determine the Fluorescence intensity of MHC in different groups; D: Semi-quantitative analysis to determine the Fluorescence intensity of MyoD in different groups; E: RT-PCR to determine the CCL-2 expressions in different groups. *$p < 0.05$, ***$p < 0.01$.

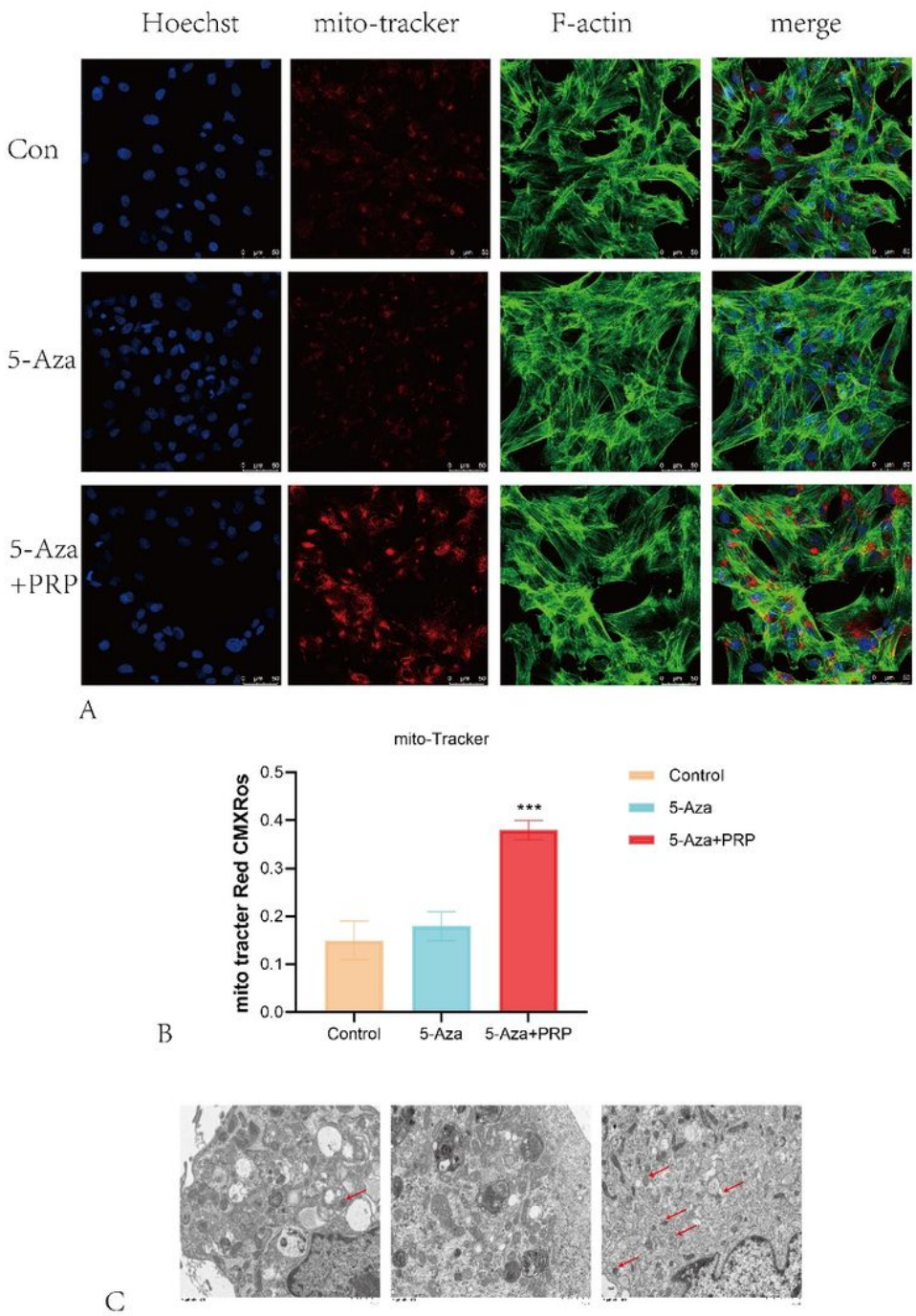


## Figure 4

**The regulatory effect of PRP on the mitochondrial function of ADSCs.** A: Mito-Tracker to determine the mitochondrial morphological change in different groups; B: Emi-quantitative analysis to determine the Fluorescence intensity of mito-Tracker Red CMXRos in different groups; C: Observation of mitochondrial autophagy bodies by transmission electron microscope. ***$p < 0.01$.

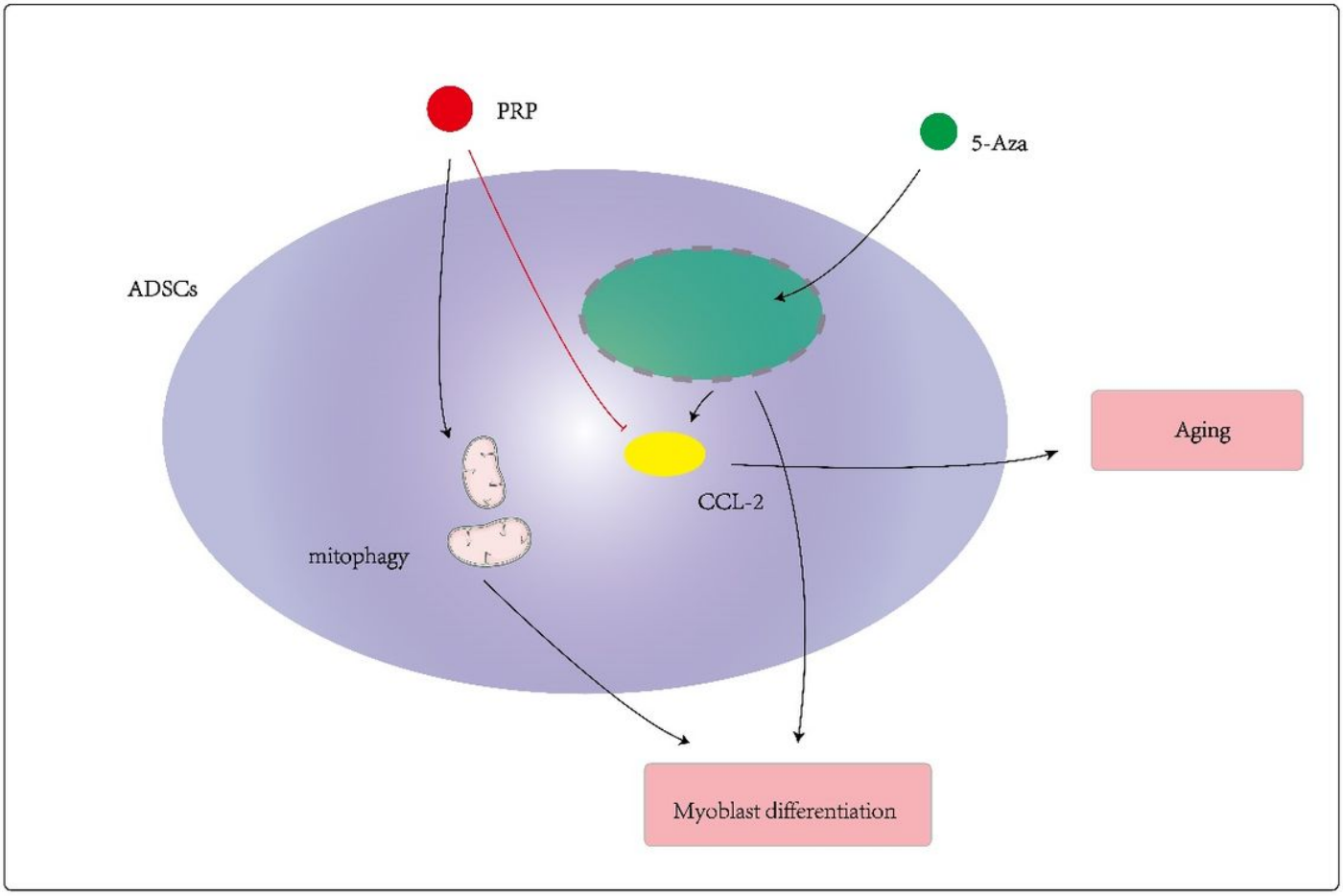


## Figure 5

**The hypotheses of this study.** PRP protect the activity of ADSCs and promote its myogenic differentiation efficiency. Meanwhile, PRP can promote mitophagy. The above functions may be caused by inhibiting the expression of CCL-2.